Effect of counterions on the spectrum of dissolved DNA polymers

V. K. Saxena and L. L. Van Zandt
Department of Physics, Purdue University, West Lafayette, Indiana 47907
(Received 14 October 1991)

The effective-field model for the dynamics of DNA polymer in solution has been extended to include the effect of monovalent counterions surrounding the polymer. The effect of site-bound counterions as compared to the area-bound counterions has been included specifically by explicitly introducing degrees of freedom for the counterions associated with a monomer and coupling these to the DNA degrees of freedom via appropriate interactions. Stability of the system for all vibrational modes was used as a criterion to find possible equilibrium positions of the site-bound counterions. The normal-mode spectrum of DNA homopolymer poly(dA)-poly(dT) with different monovalent counterion species is calculated. Based on an analysis of the eigenvectors, a mode around 25 cm^{-1} is found to have a strong plasmonlike character, i.e., a large electric dipole moment associated with longitudinal collective oscillations of the DNA-water-counterion system. Further analysis of eigenvectors with strong counterion motion gives information about effective force constants binding counterions to the polymer backbone. The effect of varying counterion species and the degree of the site-bound character of counterions was also investigated by examining the variation of frequencies of various modes with similar characteristic motions.

PACS number(s): 87.10.+e, 87.15.Mi, 82.80.Ch

I. INTRODUCTION

Infrared and Raman spectroscopic studies of DNA polymers generally give information only on the frequencies of the vibrational modes of the system. For physical interpretation and analysis in terms of atomic motion, and thereby possible biological and other applications, it is very important to have detailed information about the various types of motions involved with each individual mode. This information is contained in the respective *eigenvectors* of each mode. Unfortunately experimental *eigenvector* information is much scarcer than *eigenvalues*. A significant reasonable comparison between eigenfrequencies predicted by theoretical models and the spectroscopic observations, which normally show only fewer, broader resonances, is possible only if some details of eigenvector characteristics can be determined. This presents a relatively difficult task of identifying different modes observed in spectroscopic measurements.

In the frequency range above about 300 cm^{-1} the observed spectrum consists of many sharp, well-defined lines [1]. The frequencies of these resonances can be interpreted in terms of a model based on short-range bonded interactions, near-neighbor stretch, and angle-bend forces. These features, and consequently the corresponding resonances, generally involve motions of small numbers of atoms confined to a relatively local part of a monomer [2]. Simple adjustments of parameter values corresponding to bonded force constants serve to identify and interpret the eigenvector characteristics in this frequency range.

The situation becomes unclear in the low-frequency and millimeter-microwave range of the spectrum, a range which is, however, extremely important from the physical as well as the biological perspective [2]. In this range of frequencies a large number of degrees of freedom are involved in all the normal modes. The system dynamics may resemble that of an elastic continuum. Involvement of more or less all the atoms makes the identification of the modes more difficult. It has long been established [3] that this range of spectrum is very sensitive to weaker nonbonded long-range interactions between distant parts of the long polymer chain.

Besides the weaker, nonbonded interactions among polymer atoms, the surrounding medium also affects the behavior and motion of the molecule. The DNA polymer is a negatively charged molecule with approximately two units of negative charge on each monomer. This charged helical polymer is immersed in an ionic aqueous medium. The near neighborhood of the molecule contains excess, neutralizing, positively charged metallic counterions. Surrounding water and counterions play a very important role in stabilizing the equilibrium configuration of DNA [4]. The interactions, mainly electrostatic, of the charged counterions with the partial atomic charges on the polymer atoms unavoidably influence the dynamics of the complete system and the normal modes in detail. These counterions play important roles in processes such as structural transitions [5,6] and aggregation [7]. Soumpasis [8–11] has shown that the concentration, charge, and size of the counterions can profoundly influence the dissolved DNA polymer.

Two different approaches have been used to study the effect of long-range nonbonded forces and the surrounding layer of water, also called the hydration sheath, on the dynamics of DNA. In the earlier approach long-range forces are assumed and parametrized for all pairs of polymer atoms out to large separations. This requires dealing with a very large number of dynamical coefficients [3] ($>20\,000$). The effect of the surrounding hydration sheath is treated in terms of some phenomenological dielectric constants on these intramolcular in-

teractions [12–14]. Some scheme must be chosen to generate a dielectric constant to associate to every interacting pair.

The shortcomings of the earlier model, cited above, were at least partially overcome in the effective-field model developed for dissolved DNA polymers [15]. This approach differs from the earlier one in various aspects. First, an explicit dynamical coordinate is introduced to account for the motion of the hydration sheath. To account for the positive charges on the counterions, mostly contained within the sheath, complete charge neutrality is imposed on the sheath-polymer combination. Second, the nonbonded long-range forces, essentially electrodynamic in nature, are expressed in terms of local electric fields. These are determined from the geometry of the system, with appropriate boundary conditions, as solutions of Maxwell's equations. These fields in turn are coupled to the local partial atomic charges within a unit cell and the corresponding part of the hydration sheath. The effect of the polarizable aqueous medium is realistically included by means of a measured, frequency-dependent dielectric constant determined from independent measurements [16]. This approach has led to the prediction of a number of interesting features of the DNA normal-mode spectrum [17–19].

The positively charged counterions in the medium surrounding the charged polymer interact with the molecule in various ways. The partial atomic charges on the polymer atoms have electrostatic, direct Coulomb interactions with the counterions. The electric polarizabilities both of the counterions and the atoms on the molecule also interact via van-der-Waals–type forces. The counterions are consequently held in the near vicinity of the polymer.

Manning has suggested [20,21] that the counterions in an aqueous polyelectrolyte medium surrounding a charged polymer can be confined near the polymer in two well-established ways. In one case, called *site bound,* the counterions are in direct contact with one or more charged groups on the polymer, with little or no intervening water. The ion positions are definite. In the other case, bound counterions are restrained to remain close to the polymer, but are relatively free to shift about on its surface, hence they are called *area* bound or *territorially* bound. In the case of site-bound counterions the localization effects of the counterions are stronger than in the case of the area-bound counterions. The term area bound suggests [21] that if the counterion in its free state is slightly hydrated, as in the case of K^+, then its interactions with specific locations on the polymer will be sufficiently weak to be dominated by the overlapping Coulomb fields of the charged groups. As a consequence, the counterion will be drawn into the polymer as a whole by strong fields of the charged polymer but, once there, will be more or less free to wander about the polymer surface, encountering relatively small perturbations in its otherwise random trajectory. The definitions of two distinct classes of counterion bindings suggest that the interactions of the counterions with the DNA polymer will be different in the two cases. As a consequence of different types of counterion interaction, the effects on the vibrational mode spectrum of DNA are also expected to be different in the two cases.

Manning [21] has further argued that in solutions, site binding of counterions is in some sense exceptional and area binding will be the rule. For drier, more concentrated material, however, site binding must eventually become the dominant situation, because the area-bound ions depend on their interaction with the surrounding water to maintain their mobility. Manning's theory does not take detailed account of the ion-polymer interaction potential energy map and cannot be expected to be applicable to the regime intermediate between crystalline dry material and dilute solutions. We think it quite possible that while Manning's theory well describes many attributes of the dilute case, partial or temporary site binding of the sort we discuss here may persist into the dilute regime, and that such persistence would not conflict with Manning's arguments.

While Manning's discussions suggest the area-site binding question to represent a sharp dichotomy, we take the position here that ions may spend some time "stuck" in the dimples—local minima—of the potential surface when their energies are low, then under statistical fluctuation be excited and drift about for a time before falling back into another dimple. We introduce the continuous parameter x_c to characterize this stochastic distribution in the two states. If the dichomotomy is in fact sharp, only the values $x_c = 0, 1$ are of significance. We take this to be an experimental question answerable by measurements of frequency versus water content.

Besides the type of counterion binding, different counterion species can have different effects on the spectrum. Different species of counterions may have different degrees of binding with the polymer. All these considerations must influence the normal-mode behavior of the DNA–hydration-sheath–counterion system in a complicated manner.

Some experimental observations and spectroscopic measurements of the effect of counterions on the structure and spectrum of DNA have been reported [22–24]. Some vibrational modes have been found to be dependent on counterion species and hydration conditions of the system [25,26,23]. Some model calculations have also been performed to examine the effect of counterions on the DNA dynamics [27,28]. The calculation done by Young, Prabhu, and Prohofsky [27] extended the earlier model of pairwise long-range forces by including two counterions for each monomer. This calculation, of course, retains the weaknesses of the original on which it is based [19]. Another calculation, recently reported by Lavalle, Lee, and Flox [28], uses a very simple masses-and-springs model of coupled chains utilizing only near-neighbor elastic forces, and neglects the nonbonded long-range interactions completely. This model also omits the detailed helical structure of the DNA polymer. Both these calculations assume counterions localized on fixed sites and also assume a direct binding to specific regions of the polymer. Thus these approaches treat only the case of site-bound counterions.

The effective-field approach [15] mentioned above serves better to account for the effect of counterions, be-

cause of (1) its incorporation of the detailed helical structure of DNA, (2) the use of separate dynamical coordinates for the hydration layer, (3) realistic treatment of the dielectric response of surrounding water, and (4) an improved computational procedure [19]. However, as this approach uses a single dynamical coordinate for the hydration sheath, water, and the counterions, the only counterion-species effect it can describe is a direct mass loading of the water dynamical coordinate by the counterion masses. Further, in this calculation the charges of the counterions are effectively smeared out over the entire hydration sheath volume. This situation, in fact, corresponds to the case of area-bound counterions, as discussed above. Well-localized, site-bound counterions cannot be treated.

To date there has been to our knowledge no complete physical model estimating the effect of counterions, comparing site bound as well as area bound, on the DNA vibrational dynamics. A study of the variation of dynamical behavior with varying degrees of boundedness, that is partially site bound and partially area bound, of the counterions would seem to be very desirable. In this paper we present a model calculation of the effect of counterions, with variable binding conditions, on a dissolved DNA homopolymer. We also examine the effect of the counterion species on the DNA spectrum.

In the next section we describe the extension of the effective-field model to include the counterions, explicitly including the effect of various binding possibilities. We use the theory to calculate the low-to-intermediate-frequency spectrum of the system under various binding conditions. In Sec. III we examine the effect of various counterion species on the spectrum and other physically measurable parameters of the system. We also explore, in Sec. IV, the effect of including a direct, covalent-type coupling of the counterions with specific binding sites on the DNA polymer. The last section contains conclusions and discussion of our results and implications for experimental observations.

II. EFFECTIVE-FIELD APPROACH WITH COUNTERIONS

The effective-field approach [15,16] as mentioned earlier, takes account of the presence of counterions in the surrounding medium only through a single dynamical coordinate describing the hydration sheath with the total charge and mass smeared over the cylindrical sheath volume, and not having specific interaction with DNA atoms. This is appropriate for the case of area-bound counterions. For the case of site-bound counterions, a complete description must consider the motion of each counterion individually, and therefore only separate explicit dynamical coordinates for counterions can treat this situation. On the average, there are two (monovalent) counterions for each monomer [4]. (This usage denotes every ion necessary to achieve charge neutrality as a "counterion.")

In addition to 123 atomic coordinates of a DNA monomer and the one coordinate for the longitudinal motion of the hydration sheath, six more dynamical coordinates need to be included in the usual set of equations of motion for the system. These are, of course, the three translational degrees of freedom for each of the two counterions. To examine the effect of varying binding conditions, as discussed in the last section, we also introduce a parameter x_c, the degree of site binding. $x_c=1$ corresponds to total site binding, and $x_c=0$ the case of completely area-bound counterions. Values of x_c between 0 and 1 mean partially site-bound counterions, and may be interpreted as fractional time spent in a site-bound location.

The DNA homopolymer possesses helical symmetry. Since 1971, this symmetry has been exploited for the calculation of dynamical and other properties of the system [1]. The polymer and the associated, surrounding hydration sheath can be viewed as a one-dimensional lattice, with a unit cell containing a complete monomer. The dynamics of a dissolved DNA polymer, along with the hydration sheath and the counterions, can be described by a set of equations of motion for the dynamical coordinates of the component atoms in a unit cell. Assuming a partial site-binding condition, as a most general case, we assign the mass-weighted dynamical coordinates $\overline{\Pi}_l^{\alpha}=\sqrt{x_c M_c}\,\Pi_l^{\alpha}$ ($\alpha=x,y,x$; $l=1,2$; and M_c is the mass of a counterion; $x_c M_c$ is the average coupled site-bound mass loading to the polymer) for the motion of the two counterions within a unit cell. Π_l^{α} is the α component of the displacement vector $\mathbf{\Pi}_l$ of the counterion l. One can write the equations of motion of the system

$$-\omega^2 q_i^{\alpha}=\sum_{j,\beta} D_{ij}^{\alpha\beta} q_j^{\beta}+e_i' E_{\alpha}-i\omega\Gamma_i(\bar{s}-q_i^{\alpha}\eta_i)\delta_{iP}\delta_{\alpha z}+\sqrt{x_c}\sum_{l,\beta} F_{il}^{\alpha\beta}\overline{\Pi}_l^{\beta}\,, \tag{1}$$

$$-\omega^2\overline{\Pi}_l^{\beta}=\sqrt{x_c}\left[e'_c E_{\beta}-i\omega\Gamma(\bar{s}-\overline{\Pi}_l^{\beta}\mu_c)\delta_{\beta z}+\sum_{j,\alpha} F_{lj}^{\beta\alpha} q_j^{\alpha}\right]+x_c\sum_{l',\alpha} C_{ll'}^{\beta\alpha}\overline{\Pi}_{l'}^{\alpha}\,, \tag{2}$$

and

$$-\omega^2\bar{s}=-q^2 v_{\omega}^2\bar{s}-\lambda' E_z-i\omega\sum_i \Gamma_i(q_i^z-\bar{s}/\eta_i)\delta_{iP}-i\gamma'\omega\bar{s}-i\omega\Gamma\sqrt{x_c}\sum_l(\overline{\Pi}_l^z-\bar{s}/\mu_c)\,, \tag{3}$$

where ω is the frequency of a mode of the system. q_i^{α} [α ($=x,y,x$)] are the components of the mass-weighted displacement amplitude vector $\mathbf{q}_i$ of atom i, defined by $\mathbf{q}_i=\sqrt{m_i}\,\delta\mathbf{r}_i$, with mass m_i and the corresponding coordinate $\mathbf{r}_i$ of a monomer. Assuming only longitudinal motion of the water sheath, we represent this motion by a dynamical variable $\bar{s}=\sqrt{\alpha\rho}\,s$ where s represents the displacement amplitude of the near water sheath containing counterions. $\rho=\rho_0+2(1-x_c)M_c/a$ is the linear mass density of the sheath where ρ_0 is the linear mass density of water and M_c is the counterion mass. a is the helix rise. Note that for the total linear mass density, the terms in x_c cancel. It is instructive to compare these equations of motion with those of our earlier work [15] in

which the counterions were handled only within the water sheath.

The first term on the right of Eq. (1) contains the contributions to the dynamical matrix, within the harmonic approximation, from the bonded interactions (bond stretch, angle bend, and torsion) between polymer atoms. This term also contains contributions from the Coulomb and the van der Waals interactions between the pairs of DNA atoms within a unit cell, and contributions from the van der Waals interactions between pairs of DNA atoms within the unit cell and the nearest-neighbor cells on both sides. Collection of all these forces is contained in the force-constant matrix $D_{ij}^{\alpha\beta}$.

The third term on the right-hand side of Eq. (1) incorporates the dissipative forces at the polymer-solvent interface, with a similar term in Eq. (3), the equation of motion for the water sheath. Equation (3) also contains the term $-i\omega\gamma'\bar{s}$ for damping at the sheath-bulk water interface. The first term on the right-hand side of Eq. (3) represents the elastic contribution to the sheath motion. v_w is the sound speed in bulk water, and q the wave vector for propagation of the disturbance along the DNA-solvent system. $\eta_i \equiv \sqrt{a\rho/m_i}$. Kronecker deltas δ_{iP} and $\delta_{\alpha z}$ restrict the frictional forces at the DNA-sheath interface to the coupling of the z component of the motion of phosphorus atoms on the two backbones with longitudinal motion of the sheath. The damping parameter γ', for the sheath-bulk water coupling, is derived from the viscosity of bulk water [29]. These matters have been fully developed before [15,18,19].

The last terms on the right-hand sides of Eqs. (1) and (2) describe the motion of the counterions. The last term in Eq. (2) contains the elements $F_{lj}^{\beta\alpha}$ of the force-constant matrix of direct interactions between the counterions and the DNA polymer. A similar equal and opposite term appears in Eq. (1) for the motion of atoms in the DNA monomer. These are action-reaction pairs. We have introduced a damping term the second term in Eq. (2), between the z motion of the counterions and the motion of the water sheath. The constant Γ in this term couples the z motion of the counterions with the water. An elementary calculation based on the dc conductivity of ionic solutions shows that Γ is so large that they move together almost perfectly as if the counterions were glued to the water. $\mu_c = \sqrt{a\rho/M_c}$.

The various powers of x_c call for some explanation. x_c may be considered either a fractional occupation time of a site-binding position as mentioned before, or alternatively for a long polymer, a fraction of linked polymer sites occupied at any one time. For calculating the dynamics of collective running waves on the polymer, it is as if every site were occupied by a lighter, less stiffly bound ion. Thus the force constant appearing in Eq. (1) for ion-atom binding needs a factor x_c. In mass-weighted coordinates, all the force constants get divided by the square roots of the masses of the respective atoms. Hence the effective ion force constants get divided by the root effective mass and thus by $\sqrt{x_c}$ as well as $\sqrt{M_c}$. This is unsatisfactory, because it leaves hidden dependences of x_c in the constants of the equations of motion. Thus, instead we use $F_{il}^{\alpha\beta}$ defined without x_c in the mass denominator. The overall fractional effectiveness parameter x_c is reduced thereby to $\sqrt{x_c}$, but all x_c dependence is now explicit. Corresponding corrections occur in the terms of Eqs. (2) and (3).

The last term in Eq. (2) is the force-constant-matrix contribution arising from counterion-counterion interaction. As the two counterions, on opposite sides of the monomer, are far apart, this term involves relatively smaller contributions. For the reasons discussed in an earlier paragraph this term contains x_c for the effectiveness parameter, as it involves two counterions.

The nonbonded, long-range interactions between distant parts of the polymer and corresponding counterions on distant monomers are accounted for in terms of the effective electric field [15,16] **E** with components E_α acting on the partial atomic charges on the polymer atoms and the counterion charges within the sheath. In Eqs. (1) and (2) the local-field terms contain the scaled charges $e_i' = e_i/\sqrt{m_i}$, where e_i is the partial charge on the DNA atom i within a monomer. $e_c' = e_c/\sqrt{M_c}$ is the scaled charge on a counterion. $\lambda' = \lambda/\sqrt{a\rho}$ where $-\lambda = -\sum_i e_i - 2x_c e_c$ is the total average charge of the area-bound part of the counterions within the water sheath. As before, we have assumed complete charge neutrality within the molecule-sheath system. The Poisson-Boltzmann theory indicates that this assumption is correct to about 95%.

The radial and longitudinal electric fields E_r and E_z, as described in our earlier treatment [15], prove to be given by Bessel functions. In the case of the dissolved DNA polymer considered here the appropriate Bessel functions are Hankel functions of the first kind. The radial and longitudinal fields have the form

$$E_r(q,r) = E_1(q) H_1^1(\kappa r) \tag{4}$$

and

$$E_z(q,r) = E_0(q) H_0^1(\kappa r) , \tag{5}$$

where H are the Hankel functions. κ is given in terms of the wave vector q and frequency ω of an excitation along the polymer chain, the dielectric constant ϵ_{out}, and the dc electrical conductivity σ of the hydration sheath as

$$\kappa = (-q^2 + \epsilon_{\text{out}}\mu_0\omega^2 + i\sigma\mu_0\omega)^{1/2} . \tag{6}$$

where μ_0 is the constant of magnetostatics. The amplitudes E_1 and E_0 are determined by the boundary condition at the interface between the hydration sheath and the bulk water at $r = r_1$. These boundary conditions (for details see Saxena, Van Zandt, and Schroll [15]) give expressions for the E field amplitudes in terms of the local-polarization-density vector **P**. Finally the longitudinal and radial components of the fields are given by

$$E_z(q,\omega) = \frac{1}{\epsilon_{\text{in}}} \frac{1}{\Psi(\kappa,\omega) - 1} P_z \tag{7}$$

and

$$E_r(q,\omega)=-\frac{iqr_1}{2}\frac{1}{\epsilon_{\text{in}}}\frac{\Psi(\kappa,\omega)}{\Psi(\kappa,\omega)-1}\left[P_z+\frac{2}{iqr_1}P_r\right], \quad (8)$$

where

$$\Psi(\kappa,\omega)=\frac{2}{\kappa r_1}\frac{i\sigma+\omega\epsilon_{\text{out}}(\omega)}{\omega\epsilon_{\text{in}}}\frac{H_1^1(\kappa r_1)}{H_0^1(\kappa r_1)}, \quad (9)$$

where ϵ_{in} is the dielectric constant in the sheath region. P_z and P_r are the longitudinal and radial components of the local polarization density vector **P** which is given in terms of local atomic displacements as

$$\mathbf{P}=\frac{1}{\pi r_1^2 a}\left[\sum_i e_i\delta\mathbf{r}_i+x_c e_c\sum_l \Pi_l-\hat{\mathbf{z}}s\lambda\right]. \quad (10)$$

The effect of the surrounding aqueous medium is accounted for by means of a frequency-dependent dielectric constant and elastic properties known from the speed of sound in water [16]. The frequency-dependent dielectric function of the medium $\epsilon_{\text{out}}(\omega)$ is given by [30]

$$\epsilon_{\text{out}}(\omega)=\frac{\epsilon_{\text{dc}}-\epsilon_\infty}{1+i\omega\tau_s}+\epsilon_\infty, \quad (11)$$

where ϵ_{dc} and ϵ_∞ are the zero-frequency static dielectric constant and infinite-frequency dielectric constant of the aqueous medium, respectively. τ_s is the dielectric relaxation time of the solvent medium, 7.9×10^{-12} sec from the most recent value reported from microwave absorption measurements [31]. This gives the range of most rapid variation of ϵ_{out} around 50–100 cm^{-1}. Again, these matters have been described earlier [15,18,19].

The frequency dependence of the local-field terms and the damping terms renders the set of Eqs. (1)–(3) nonlinear in ω^2 and makes them difficult to solve by direct diagonalization. We have calculated the spectrum of the *B*-form homopolymer poly(dA)-poly(dT) DNA within this model using an iterative procedure to get self-consistent eigenmode frequencies and corresponding eigenvectors for each of the modes separately. From the spectroscopic point of view (ir absorption) one needs to calculate the normal-mode spectrum only at the zone center $\theta=0°$ and at $\theta=36°$ where $\theta=qa$ is the phase angle. For the frequency-independent parts of the force constant matrix $D_{ij}^{\alpha\beta}$, the damping coefficients, the sound speed for bulk water, and the values of σ and r_1 in the effective field terms we used the same set of values as in our earlier calculation [16]. Brillouin scattering studies of DNA and its hydration shell [32] show that the dielectric relaxation time within the first hydration shell is 4.0×10^{-11} sec. In accord with this in Eqs. (7)–(9) we have used a value of $2.0\epsilon_0$ for ϵ_{in}, the dielectric permittivity of the cylindrical region containing the DNA helix and the primary hydration sheath. In Eq. (11) for ϵ_{dc} we have used a value of $68.0\epsilon_0$ corresponding to water with a counterion concentration [33] of about 15%. ϵ_∞ was taken to be $1.77\epsilon_0$ from the optical index of refraction.

One important and difficult step in adding the counterions, in the site bound case, to the DNA–hydration-sheath system is to determine their equilibrium, site-bound positions relative to the set of coordinates used for the DNA [34]. There have been a number of papers involving this question. Recently in molecular-dynamics simulations of DNA with counterions, Osman, Miaskiewicz, and Weinstein [35] placed counterions at positions bifurcating the *O*—*P*—*O* angle at a distance of 5.0 Å from the phosphorus. The model used by Lavalle, Lee, and Flox [28] does not use the position coordinates for the counterions. Young, Prabhu, and Prohofsky [27] placed the sodium ions a distance of 2.7 Å away radially outward from the free phosphate oxygens, matching it to calculations by Clementi and Corongiu [36]. In this scheme the counterions are about 11.9 Å away from the axis of the double helix, within the water of the hydration sheath.

Using similar positions for counterions like those of previous authors with our set of coordinates for DNA we encountered unstable dynamics (negative eigenvalues ω^2 for the dynamical solution of the vibration problem). Such negative values for ω^2 indicate instabilities, implying an inappropriate choice of equilibrium coordinates. The associated eigenvectors showed clearly it was the ion positions which were unstable. Thus these positions were modified. We ran repeated calculations of the eigenvalue problem, for various values of the phase angle θ, and with different possible equilibrium positions for the counterions, discarding all trials giving instabilities in the normal-mode spectrum. Final equilibrium positions were found when, with all the possible interactions included, there were no negative eigenvalues. We find, contrary to the assumptions of Young, Prabhu, and Prohovsky [27] that the counterions have equilibrium positions near the surface of the polymer halfway *between* phosphate groups. In order to show the relative positions of the counterions a stereo view of a two-monomer section of the DNA with the corresponding counterions is presented in Fig. 1. A closer examination of the counterion configuration shows that the counterions just fit in the little pockets formed by the bends of the backbone carbon chain. This puts them approximately 3.0 Å away from the two dioxy (or "free") phosphate oxygens on the backbone of the monomer and also about the same distance from the oxygens in the neighboring monomers on opposite sides. Their radial distance from the axis of the helix is 9.7 Å. Moving the assumed counterion equilibria in any direction from these positions causes instabilities in the form of negative eigenvalues whose eigenvectors indicate free movements toward the stable equilibrium positions. Dislocations of the counterions around their equilibrium positions allow only a tiny volume of stability ($\sim$0.01 Å in any direction). The equilibrium coordinates of the counterions, determined as described above, along with the coordinates of free phosphate oxygens of cell 0, are listed in Table I.

The next step in including the counterions explicitly in the effective-field approach is to determine the type of interactions between the counterions and the DNA polymer atoms. These interactions are responsible for the counterion binding. The interactions to be included (in descending order of magnitude) are the following. (i) Coulomb interactions between counterions and partial

atomic charges on the DNA atoms. We have included Coulomb interactions of the counterions with all the atoms in the central monomer (cell 0) and in the nearest-neighbor monomers on either side of the central cell. (ii) We have also included van der Waals interactions between counterions and all the atoms in the central and in the nearest-neighbor cells. The contributions to the dynamical force-constant matrix coming from all these interactions are included in terms $F_{jl}^{\alpha\beta}$ in Eqs. (1) and (2). The long-range electrostatic interactions of the counterions with the atoms in distant monomers on the chain are accounted for, as for the polymer itself, in the effective field E. In evaluating the counterion-DNA contributions to the Coulomb and van der Waals interaction in the dynamical matrix we have used the same set of parameters, dielectric constants and van der Waals parameters, as for the original interactions in DNA-sheath system [15]. Young, Prabhu, and Prohofsky [27] included Coulomb, Van der Waals, and long-range interactions (by directly summing several thousand pairwise parametrized Coulomb terms) but used the usual absolute value signs around each contribution, thus effectively turning every partial atomic charge positive and changing the short-distance attractive parts of the van der Waals interactions into repulsive form. Lavalle, Lee, and Flox [28] did not use any Coulomb, van der Waals, or long-range interactions at all and replaced all the counterion interactions with the polymer by an approximate phenomenological spring constant between the counterions and the nearest phosphate groups in the polymer backbones.

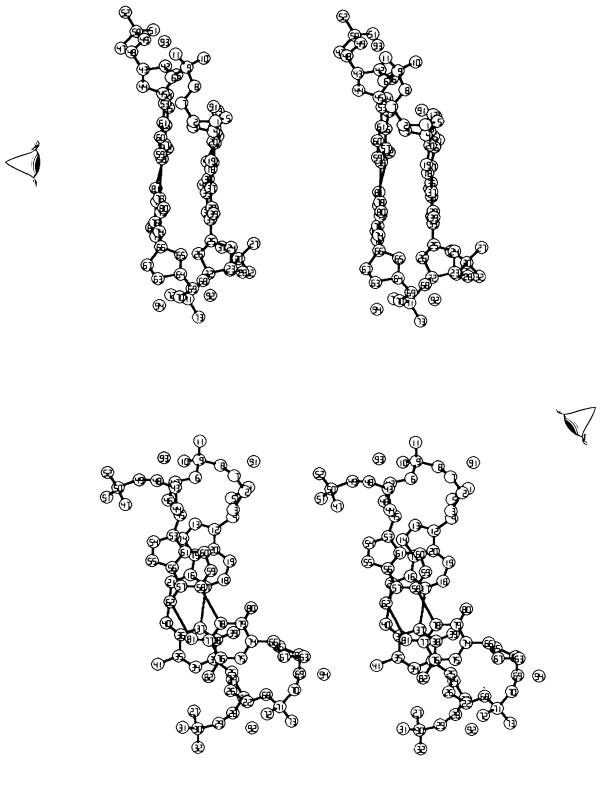

FIG. 1. Two stereo views of a two-monomer section of poly(dA)-poly(dT) DNA polymer along with four counterions. Atoms numbered 1 to 82 belong to the DNA and those numbered 91 to 94 are the counterions. The counterions are shown in their only stable sites. The vantage point of the top view is "edge on," looking perpendicular to the polymer axis, about 85° to the long axis of the base pairs. The other view is looking down along the polymer axis. Observing eyes indicate the aspects of the other view in the figure.

TABLE I. Coordinates of Na^+ counterions and the respective free phosphate oxygens on the two backbones of a *B*-conformation poly(dA)-poly(dT) DNA polymer.

Atom (or ion)	x (Å)	y(Å)	z(Å)
O (phos.)	−1.337	9.153	0.739
O (phos.)	−0.316	10.489	2.603
Ion	3.300	9.130	−0.009
O (phos.)	−1.337	−9.153	−0.739
O (phos.)	−0.316	−10.489	−2.603
Ion	3.300	−9.130	0.009

Finally, (iii) counterions may also undergo weak covalent-type binding with some of the DNA atoms. For example, depending on the size of the ion core, the outermost *s*-electron shell of a counterion may hybridize with the *s*-*p* electron shells of the free phosphate oxygens, thus giving rise to a weak (because the equilibrium distance of the counterions from these oxygens, as found from our analysis, is approximately 3.0 Å) covalent binding. This weak covalency is similar to what occurs between proton electron states and *s*-*p* shells of acceptor atoms in forming a H bond. The counterions, having a hydrogen-like outer state structure, may give rise to a very weak hydrogen-bond-like coupling with the free oxygens. In the calculations presented here we have emphasized the nonbonded forces for most of our analysis. However, since ion species dependent spectral shifts have been reported, and since these covalencies are the only possible chemistry-dependent interactions available, we have also calculated the spectra including a weak (0.1 m dyn/Å) coupling constant to each free oxygen. Allowing for the geometry of the linkages (Fig. 1) this gives a total of 0.2 m dyn/Å for each counterion. This matches reasonably well the direct-coupling free force constant of 0.35 m dyn/Å used by Lavalle, Lee, and Flox [28]. We will see later that the two parametrizations turn out to be even closer than this would suggest.

Another important parameter in the calculation of DNA spectra is the relative humidity and the structural conformation of the sample considered. Young, Prabhu, and Prohofsky [27] have performed their calculations for a relatively wet material in *B*-conformation poly(dA)-poly(dT). On the other hand Lavalle, Lee, and Flox [28] considered a crystalline sample with low relative humidity and did not take the detailed structure of the system into account. However they tried to examine the *A* to *B* transition using approximate spring force constants for interhelical interactions and varying these with relative humidity. In our calculations here, we have considered dissolved DNA polymer in the dilute limit. As at this dilution the relative humidity is large, we have done our calculations only for a *B*-conformation poly(dA)-poly(dT)

DNA. We are presently extending our model to relatively drier samples where interhelical interactions are expected to play an important role.

III. DNA SPECTRUM WITH COUNTERIONS

Once all the steps discussed in the last section are completed for the addition of counterions to the DNA–hydration-sheath system, one can calculate the complete spectrum under various physical situations of interest. In order to contrast the effect of site-bound and area-bound counterions, we performed iterative calculations for the lowest 36 modes of a *B*-conformation poly(dA)-poly(dT) DNA polymer with Na^+ counterions. We also investigated the effect of partial site binding $(0<x_c<1)$ of counterions on the DNA spectrum for Na^+. All these calculations were done using only the nonbonded interactions between counterions and DNA atoms. The effect of a direct weak covalent-type binding between counterions and the respective free phosphate oxygens was subsequently examined. This effect was calculated only for the complete site-binding situation $(x_c=1)$.

In all these cases we tried to classify vibrational modes according to similar eigenvector characteristics, representing similar motions of the various parts of the system. In particular five different characteristic motions of DNA–hydration-sheath–counterion system were used to identify and compare the several vibrational modes. This was achieved by constructing standard eigenvectors [19] for these motions and projecting the eigenvectors obtained in the calculations onto these standard eigenvectors. These standard motions are propeller twist, baseroll, hydrogen-bond breathing mode, base shift (for details of definition of these motions see Ref. [19]), and collective plasmon motion which is characterized by small, in-phase oscillations of the partial atomic charges, along with large electric fields and dipole moments [17].

Besides this, the modes with strong counterion motions were also identified. The normal mode frequencies below 200 cm^{-1}, for different values of x_c, and for the case of covalent binding included, are listed in Table II. To show the variation of mode frequencies under various situations we have tried to list the modes with similar characteristic motions in the same row. This is the reason that in Table II columns 1 through 3 list the frequencies in ascending order, but the frequencies listed in column 4 for $x_c=0.0$ and in column 5 for covalent binding do not have uniform ascending order.

An examination of Table II shows that most of the vibrational modes in this range are affected to some degree by the conditions of binding of the counterions. Frequencies of some modes are changed little by variation of x_c. Most interestingly the frequencies of the modes with similar characteristic motions for the total site binding and total area binding can differ greatly. In the case of totally area-bound counterions we have effectively a mass and charge loading of the dynamical coordinate for the hydration sheath motion, confined to the z direction. For total or partial site binding the transverse (or radial) motions of the counterions also enter the dynamics of the system as separate entities. The frequencies in the last column of Table II correspond to total site binding and a weak covalent binding with free phosphate oxygens. These frequencies, once more for some modes with similar characteristic motions, are found to differ from those without covalent binding.

For $x_c=1.0$ the mode at 24.83 cm^{-1} has a large longitudinal dipole moment characteristic of collective charge oscillations and also has a considerable projection onto the standard vector for a plasmon [17]. Thus this mode is identified as a modified plasmon of the DNA–hydration-sheath–counterion system for a complete site-binding situation. The frequency of this mode changes with varying x_c. For the case of totally site-bound counterions with a weak covalent binding this mode has a frequency of 27.05 cm^{-1}. On the other hand,for completely area-bound counterions the frequency of this mode drops to zero. A nonzero plasmon frequency for site-bound counterions and the vanishing of this frequency for area binding can be explained in terms of effective dimensionality of the system. For total area binding there is only longitudinal collective motion of the charges on the DNA atoms and the smeared charge of counterions in the sheath, which effectively gives a one-dimensional character to the oscillations. Thus the plasmon frequency is expected to vanish at the zone

TABLE II. Zone center ($\theta=0$) normal-mode frequencies (cm^{-1}) of a dissolved *B*-conformation poly(dA)-poly(dT) DNA polymer with Na^+ counterions for various values of the parameter x_c for the site binding of counterions. The last column shows the frequencies of the same system with total site binding $(x_c=1)$ with a weak covalent bonding with free phosphate oxygens.

$x_c=1.0$	$x_c=0.8$	$x_c=0.4$	$x_c=0.0$	Covalent bond
4.15	4.07	3.92	3.51	4.32
5.64	5.77	5.89	3.96	6.75
14.12	14.42	14.56	6.16	14.53
15.79	16.10	16.38	14.72	15.99
17.88	17.65	17.15	16.74	19.65
19.87	19.71	19.18	18.61	21.51
24.83	26.30	28.74	00.00	27.05
30.11	30.45	31.32	30.01	30.52
43.61	43.66	43.69	41.67	43.73
50.41	49.96	48.42	56.93	51.36
59.22	58.84	57.96	43.40	61.07
68.33	66.80	61.22	50.56	76.32
73.03	72.36	71.25	71.05	71.32
81.97	82.22	82.25	86.75	88.38
84.53	84.41	84.38	90.04	91.38
122.28	121.36	113.95	00.00	134.25
125.29	124.99	122.42	126.80	140.80
132.96	132.85	132.90	135.80	145.67
140.23	139.23	135.70	142.12	140.93
152.79	149.50	143.62	00.00	190.32
162.82	161.80	152.37	00.00	167.61
170.29	169.35	166.51	165.15	171.51
175.19	172.93	169.98	00.00	197.52

center [17,37]. On the contrary for the site-bound counterions some weak transverse motion of counterions is also associated with otherwise longitudinal collective oscillations of the system, giving an effective dimensionality 3 to the system, giving rise to a gap, a nonzero frequency at the zone center. For the site-bound counterions transverse components of interactions become comparable to the longitudinal ones, and this gives rise to a measurable transverse polarization. Although the frequency of this plasmon mode increases with decreasing x_c the projection of its eigenvector onto the standard plasmon vector, and therefore its plasmon character, somewhat decreases with decreasing x_c. For values of $x_c > 0.5$ the mode around 5.6 cm^{-1} also shows a weak component of plasmon character.

For complete site binding (column 1 of Table II) the eigenvector for the mode at 43.61 cm^{-1} shows a strong base roll component. For other values of x_c the frequencies listed in the same row also possess strong base roll motion. These frequencies, except in complete area binding, do not show much variation with change in x_c or inclusion of covalent bonding.

Other modes showing weaker base roll motion are at (for $x_c = 1.0$) 59.22 and 162.82 cm^{-1}. The mode at 50.41 cm^{-1} has a strong propeller twist motion and the modes in this row show a similar behavior. This mode shows relatively larger variation with x_c. The mode at 152.79 cm^{-1} shows weaker propeller twist motion. Besides this some other modes also have some weak propeller twist motion components. The 15.79 cm^{-1} mode shows a strong base motion along the *C*6-*C*8 long axis of the base pair. Four modes around this mode, i.e., at 5.64, 14.12, 17.88, and 19.87 cm^{-1} also show weaker similar base motions. All these modes show some modest variation with changing x_c.

The eigenvector of the mode at 73.03 cm^{-1} shows strong hydrogen-bond-breathing (HB) character. The frequency of this mode does not change much with varying x_c. The next mode, with somewhat weaker HB, is at 170.29 cm^{-1}. Besides this the four modes at 59.22, 68.33, 81.97, and 84.53 cm^{-1} also show weaker HB components. The frequencies of the modes corresponding to the 68.33-cm^{-1} mode show relatively bigger variation with x_c.

In column 4 of Table II, for $x_c = 0.0$ some of the rows list frequencies as 0.00. These frequencies correspond to the modes with strong counterion motions. As mentioned in Sec. II, inclusion of counterions introduces six new degrees of freedom to the system. As long as some site binding of the counterions is involved, these degrees of freedom appear as dynamical coordinates and consequently give rise to some modes with counterion motion indicated. For the case of completely area-bound counterions these degrees of freedom and the respective dynamical variables disappear from the physics. It is, therefore, expected that for $x_c = 0.0$ the calculation should result in six zero-frequency modes for these no longer significant, decoupled degrees of freedom. These zero-frequency modes should appear at any value of the phase angle θ. However at the zone center, $\theta = 0.0$ these zeros will be found in addition to the two zero-frequency acoustic modes of the DNA polymer and one zero-frequency mode for the collective plasmon mode. We encountered exactly nine zero-frequency modes from our calculations for $x_c = 0.0$ at the zone center. For any nonzero value of x_c six nonzero frequency modes with relatively strong counterion motion should appear. Analyzing the eigenvectors of our calculations in terms of standard vectors for counterion motions, indeed reveals six modes with these characteristics. Four of these modes, with corresponding zero-frequency modes for $x_c = 0.0$, are listed in columns 1 through 3 and in column 5 of Table II. As the counterions are part of the full complete system, it is not possible to separate the modes into classes with pure x motion or pure y motion of counterions. However projecting the eigenvectors onto the standard vectors one can have an idea about the nature of motion involved. The four modes listed at 122.28, 152.79, 162.82, and 175.19 cm^{-1} show substantial radial counterion motion with substantial x or y components. As is expected with the addition of weak covalent binding all these modes rise in frequency, as shown in column 5 of Table II. Besides the four modes, we found two more modes, not listed in Table II, with strong counterion motion components at 218.05 and 287.72 cm^{-1}

We use the mode frequencies showing the strongest radial counterion motion to estimate an effective force constant for the counterion-DNA binding. We calculate an effective force constant as $M_c\omega^2$. We thereby obtained a value of 0.28 mdyn/Å. Thus we sustain the value 0.35 mdyn/Å as used by Lavalle, Lee, and Flox [28] in their reduced dimensionality calculation. We believe our values here give a firm first-principles basis to their parameter choice.

The normal modes of the system can be characterized, at least in part, in terms of infrared and Raman activities of the lines. The infrared activity of a spectral line is proportional to the transition dipole moment of the line. To complement the characterization of modes presented in the preceding paragraphs, in Table III we present the perpendicular ($I_\perp$), parallel ($I_\parallel$), and the total (I_t) infrared activities of all the zone center ($\theta = 0$) modes below 200 cm^{-1} of a homopolymer with site-bound ($x_c = 1$) Na^+ counterions. Predicting Raman intensities is more difficult. We are at work on this problem.

We also performed calculations of the DNA spectrum for different counterion species. Specifically we used four counterions, Na^+, K^+, Rb^+, and Cs^+. Although we did various calculations for different values of the binding parameter x_c, in Table IV we list the zone center normal-mode vibrational frequencies only for the case of completely site-bound counterions. This should be the case showing greatest contrast between the various counterions. As can be seen from Table IV the frequencies of most of the modes are affected by counterion size and mass. In particular some of the modes, like the plasmon mode and the modes with relatively larger counterion-motion components, are quite sensitive to the counterion species. The general trend is that most of the modes soften with increasing counterion size and mass. By con-

TABLE III. Perpendicular ($I_\perp$), parallel ($I_\parallel$), and total (I_t) infrared activities at the zone center ($\theta=0$) for modes below 200 cm^{-1} for site bound ($x_c=1$) Na^+ DNA.

ω (cm^{-1})	$I_\perp$	$I_\parallel$	I_t
4.15	0.0059	0.0020	0.0062
5.64	0.0092	0.0605	0.0612
14.09	0.0417	0.0149	0.0443
15.78	0.0307	0.0124	0.0331
17.88	0.0212	0.0085	0.0231
19.86	0.0216	0.0306	0.0375
24.83	0.0587	0.2172	0.2250
30.09	0.0439	0.0699	0.0825
43.61	0.0340	0.0271	0.0434
50.40	0.0677	0.0566	0.0882
59.21	0.0343	0.0255	0.0427
68.33	0.0672	0.0459	0.0814
73.02	0.0364	0.0193	0.0412
81.95	0.0713	0.0176	0.0735
84.53	0.0562	0.0675	0.0879
122.27	0.1292	0.0387	0.1349
125.28	0.1068	0.0203	0.1087
132.96	0.0525	0.0038	0.0527
140.23	0.1449	0.0016	0.1449
152.78	0.2552	0.0032	0.2553
162.81	0.0765	0.2070	0.2207
170.26	0.0120	0.0321	0.0343
175.19	0.0772	0.0901	0.1186

TABLE IV. Zone center ($\theta=0$) normal-mode frequencies (cm^{-1}) of a dissolved *B*-conformation poly(dA)-poly(dT) DNA polymer with different species of site-bound ($x_c=1$) monovalent counterions.

Na^+	K^+	Rb^+	Cs^+
4.15	3.99	3.62	3.33
5.64	5.42	4.96	4.66
14.12	14.03	13.79	13.56
15.79	15.54	15.01	14.61
17.88	17.56	16.74	16.06
19.87	19.42	18.39	17.62
24.83	22.92	20.13	18.83
30.11	29.90	29.69	29.60
43.61	43.50	43.28	43.11
50.41	49.84	48.68	47.90
59.22	58.56	56.77	54.32
68.33	63.01	57.53	56.30
73.03	71.82	70.10	68.79
81.97	79.66	74.26	71.18
84.53	82.55	78.83	75.82
122.28	113.09	100.35	96.72
125.29	119.58	106.14	100.13
132.96	131.68	129.74	128.53
140.23	136.08	133.55	133.01
152.79	146.05	140.73	138.92
162.82	153.40	146.28	145.37
170.29	167.23	166.10	165.49
175.19	179.30	170.18	170.05

trast, comparison of normal-mode frequencies for different counterion species of a complete area-binding situation shows little variation in mode frequencies with counterion mass and size. This is because in the case of completely area-bound counterions the effect of the counterions can only be a mass loading of the sheath dynamics. As the mass of the water sheath within a unit cell is already large compared to the mass of any counterion, the overall effect is correspondingly small. The sheath involves approximately 30 water molecules per monomer. Further, in case of area-bound counterions the detailed Coulombic and van der Waals interactions between individual counterion and the DNA atoms cease to exist, at least in the present model, and the effect of changing counterion species turns out to be very small.

The dependence of the frequencies (of any mode) on counterion species will be a measure of the extent to which the counterions are site bound or area bound, and serves as a direct experimental test of this parameter (x_c).

Analyzing the compressional-mode frequencies for very low phase angle θ enabled us to calculate the compressional-wave sound speed of the DNA–hydration-sheath–counterion system. The values of the calculated sound speed for the four counterion species in two different limits $x_c=1.0$ and 0.0 are listed in Table V. From this table one can see that the sound-wave speed for completely site-bound counterions is sensitive to the counterion species and decreases with increasing counterion size and mass. On the other hand the sound speed for completely area-bound case, with an effective mass loading of the sheath dynamical coordinate, is practically independent of the counterion type.

The results of our calculation for completely or partially site-bound counterion species are very much in accord with recent experimental findings [22]. A so-called "25-cm^{-1}" mode has recently been observed in some DNA samples at relatively lower humidity conditions [26,23]. This mode has been interpreted as arising due to interhelical interactions, mediated by counterions, since it is found in drier samples with necessarily neighboring polymer chains. This mode is also found to depend, although weakly, on the counterion species. In our calculations we find a mode in the 25-cm^{-1} range for completely site-bound counterions. The frequency of this mode, as shown in Table IV, varies with changing counterion size and mass. An interesting and important feature observed in our calculations is the plasmon nature of this mode. Our results are valid mainly for materials with large water content, and include no interhelical interactions.

TABLE V. Sound speed (km/s) for a dissolved *B*-conformation poly(dA)-poly(dT) DNA polymer with different species of monovalent counterions in two different limits $x_c=0$ and 1 of binding.

Ion	$x_c=1.0$	$x_c=0.0$
Na^+	1.85	2.12
K^+	1.80	2.12
Rb^+	1.66	2.11
Cs^+	1.53	2.11

However, the presence of a strongly polar mode near 25 cm^{-1} and its dependence on counterion species in our calculations indicates that the mode observed experimentally in this range may well be a collective plasmon mode of the combined DNA–hydration-sheath–counterion system. This is an interesting alternative to the interhelical-mode hypothesis.

Wittlin *et al.* [38] have observed a strong mode in the infrared absorption at around 40 cm^{-1}. Their experiments were performed on drier materials than we dare to apply this theory to. As we have mentioned, with increasing water content the plasmon frequency at $q=0$ eventually sinks to zero, and is still rising as we move toward the driest conditions appropriate for this theory. Wittlin's measurements are therefore not inconsistent with this theory, although we hesitate to make any stronger statement. It should also be noted that the 25-cm^{-1} line is observed in Raman scattering, and we have only given the infrared activity. In materials showing inversion symmetry, Raman and infrared activity are mutually exclusive. DNA, of course, is strongly right-handed, and the exclusion theorem does not apply. Nonetheless, we appreciate the need for a theory of Raman intensities to complement the (considerably less difficult) theory of infrared activity we have given. This theory is under development.

Weidlich, Lindsay, and Rupprecht [22] have measured the counterion species and concentration dependence of the low-frequency Raman spectrum and speed of sound in solid DNA samples. The variation of the speed of sound with counterion species calculated in the present model conforms to that found by these authors. Our calculations were done for wetter material, consequently giving considerably lower values for the speed of sound, as compared to the experiments. The strong drop in sound speeds with increasing humidity is a well-known effect [39], and our sound speed values are consistent with measured values in the high humidity range. The approximate fractional magnitude of the calculated shift with changing counterion species is in agreement with Weidlich's data. The same authors also found softening of most of the modes, through decreasing Raman shifts, with increasing counterion mass and size. This is also in accord with the behavior of most of the modes listed in Table IV.

There are more aspects to compare between this calculation and the experiments than there are with the other calculations. First, Young, Prabha, and Prohofsky [27] considered only one type of counterion Na^+ and only a completely site-bound counterion system. These authors also did not include the dynamics of the hydration sheath. However they did obtain an overall shift in the frequencies of many of the millimeter microwave modes on adding counterions. Second, the calculations of Lavalle *et al.* mainly concentrated on the 25-cm^{-1} mode and found the frequency of this mode to decrease slowly with increasing counterion size. As far as both calculations overlap with ours, they are in substantial qualitative agreement; it is in the quantitative details that the differences we have discussed manifest themselves.

IV. CONCLUSIONS AND DISCUSSION

We have developed a model calculation to study the effect of counterion binding and species on the millimeter-microwave spectrum of dissolved DNA polymers, taking into account the dynamics of the surrounding aqueous hydration sheath. Our calculations lead to results very much in accord with existing experimental findings. We find that the frequencies of many modes in this range are sensitive to the type of counterion binding, site bound or area bound, and also the size and mass of the counterions. One interesting result is the existence of a plasmon mode around 25 cm^{-1}, which coincides with a mode found in solid DNA samples. The Raman activity of the 25-cm^{-1} mode has been established experimentally. This model predicts that for the appropriate hydration regime this mode should also exhibit substantial infrared activity. If this holds true, we suggest that this experimentally observed mode may then be interpreted as a collective plasmon mode with a large associated electric dipole moment. We also suggest that the variation of mode frequencies with counterion binding and species may probably be used as a technique for identifying some of the normal modes of the system. Contrary to earlier suggestions by some authors [22] we find that intrahelical modes, below 35 cm^{-1}, are also influenced by counterion effects.

Our model was developed for samples with large relative humidity, in that there are no interhelical effects included. As mentioned, the proper x_c value may be a humidity-dependent matter. There have been suggestions that interhelical interactions in relatively drier samples may play important roles and may be responsible for structural transitions. We are extending our model to situations with a finite density of DNA chains with interchain interactions.

ACKNOWLEDGMENT

This work was performed under the Office of Naval Research (ONR), Contract No. N00014-91-1703.

[1] E. W. Small and W. L. Peticolas, Biopolymers **10**, 1371 (1971).
[2] V. K. Saxena, L. L. Van Zandt, and W. K. Schroll, Chem. Phys. Lett. **164**, 82 (1989).
[3] W. N. Mei, M. Kohli, E. W. Prohofsky, and L. L. Van Zandt, Bipolymers **20**, 833 (1981).
[4] W. Saenger, *Principles of Nucleic Acid Structures* (Springer-Verlag, New York, 1984).
[5] D. W. Gruenwedel, C.-H. Hsu, and D. S. Lu, Biopolymers **10**, 47 (1971).
[6] F. M. Pohl and T. M. Jobin, J. Mol. Biol. **67**, 375 (1972).
[7] M. G. Fried and V. A. Bloomfield, Biopolymers **23**, 2141 (1984).
[8] D. M. Soumpasis, Proc. Natl. Acad. Sci. U.S.A. **81**, 5116

(1984).
[9] D. M. Soumpasis, in *Biomolecular Stereodynamics IV,* edited by R. H. Sarma and M. H. Sarma (Adenine, New York, 1986), p. 47.
[10] D. M. Soumpasis, J. Wiechen, and T. M. Jobin, J. Biomol. Struct. Dyn. **4**, 535 (1987).
[11] D. M. Soumpasis, M. Robert-Nicoud, and T. M. Jobin, Fed. Eur. Biochem. Soc. Lett. **213**, 341 (1987).
[12] V. V. Prabhu, W. K.Schroll, L. L. Van Zandt and E. W. Prohofsky, Phys. Rev. Lett. **60**, 1587 (1988).
[13] V. V. Prabhu, L. Young, and E. W. Prohofsky, Phys. Rev. B **39**, 5436 (1989).
[14] L. Young, V. V. Prabhu, and E. W. Prohofsky, Phys. Rev. A **40**, 5451 (1989).
[15] V. K. Saxena, L. L. Van Zandt, and W. K. Schroll, Phys. Rev. A **39**, 1474 (1989).
[16] V. K. Saxena and L. L. Van Zandt, Phys. Rev. A **42**, 4993 (1990).
[17] L. L. Van Zandt and V. K. Saxena, Phys. Rev. Lett. **61**, 1788 (1988).
[18] L. L. Van Zandt and V. K. Saxena, Phys. Rev. A **39**, 2672 (1991).
[19] V. K. Saxena, B. H. Dorfman, and L. L. Van Zandt, Phys. Rev. A **43**, 4510 (1991).
[20] G. S. Manning, Q. Rev. Biophys. **11**, 179 (1978).
[21] G. S. Manning, Acc. Chem. Res. **12**, 443 (1979).
[22] T. Weidlich, S. M. Lindsay, and A. Rupprecht, Phys. Rev. Lett. **61**, 1674 (1988).
[23] T. Weidlich, S. M. Lindsay, Qi Rui, A. Ruppecht, W. L. Peticolas, and G. A. Thomas, J. Biomol. Struct. Dynam. **8**, 139 (1990).
[24] N. Lavalle, S. A. Lee, and A. Rupprecht, Biopolymers **30**, 877 (1990).
[25] S. A. Lee, S. M. Lindsay, J. W. Powell, T. Weidlich, N. J. Tao, G. D. Lewen, and A. Ruppect, Biopolymers **26**, 1637 (1987).
[26] T. Weidlich and S. M. Lindsay, J. Phys. Chem. **92**, 6479 (1988).
[27] L. Young, V. V. Prabhu, and E. W. Prohofsky, Phys. Rev. A **39**, 3173 (1989).
[28] N. Lavalle, S. A. Lee, and L. S. Flox, Phys. Rev. A **43**, 3126 (1991).
[29] B. H. Dorfman and L. L. Van Zandt, Biopolymers **23**, 913 (1984).
[30] R. Pethig, *Dielectric and Electronic Properties of Biological Materials* (Wiley, New York, 1979).
[31] H. R. Garner, A. C. Lewis, and T. Ohkawa (unpublished).
[32] N. J. Tao, S. M. Lindsay, and A. Rupprecht, Biopolymers **27**, 1655 (1988).
[33] J. B. hubbard, L. Onsager, W. M. Van Beek, and M. Mandel, Proc. Natl. Acad. Sci. U.S.A. **74**, 401 (1977).
[34] R. Chandrasekaran and S. Arnott, in *Numerical Data and Functional Relationship in Science and Technology,* edited by W. Saenger, Landolt-Börnstein, New Series, Group X, Vol. VII, Pt. 1b (Springer-Verlag, Berlin, 1989).
[35] R. Osman, K. Miaskiewicz, and H. Weinstein, J. Biomol. Struct. Dyn. **8**, a159 (1991).
[36] E. Clementi and G. Corongiu, IBM DPPG Research Report No. POK-1 (unpublished).
[37] A well-illustrated discussion appears in W. A. Harrison, *Solid State Theory* (McGraw-Hill, New York, 1970).
[38] A. Wittlin, L. Genzel, F. Kremer, S. Háseler, A. Poglitsch, and A. Rupprecht, Phys. Rev. A **34**, 493 (1986).
[39] M. B. Hakim, S. M. Lindsay, and J. Powell, Biopolymers **23**, 1185 (1984).